Proton-Sponge Coated Quantum Dots for siRNA Delivery and Intracellular Imaging

ARTICLE *in* JOURNAL OF THE AMERICAN CHEMICAL SOCIETY · AUGUST 2008

Impact Factor: 12.11 · DOI: 10.1021/ja800086u · Source: PubMed

5 AUTHORS, INCLUDING:

Max Yeslev
Vanderbilt University
27 PUBLICATIONS **1,550** CITATIONS
SEE PROFILE

Shuming Nie
Emory University
212 PUBLICATIONS **35,154** CITATIONS
SEE PROFILE

Published in final edited form as:
J Am Chem Soc. 2008 July 16; 130(28): 9006–9012. doi:10.1021/ja800086u.

Proton-Sponge-Coated Quantum Dots for siRNA Delivery and Intracellular Imaging

Maksym V. Yezhelyev[1], **Lifeng Qi**[2], **Ruth M. O'Regan**[1], **Shuming Nie**[1,3,*], and **Xiaohu Gao**[2,*]

1*the Winship Cancer Institute, Emory University, Atlanta, GA 30322, USA*

2*Department of Bioengineering, University of Washington, William H Foege Building N530M, Seattle, WA 98195, USA*

3*the Department of Biomedical Engineering and Chemistry, Emory University and Georgia Institute of Technology, 101 Woodruff Circle, Suite 2001, Atlanta, GA 30322, USA*

Abstract

We report the rational design of multifunctional nanoparticles for short-interfering RNA (siRNA) delivery and imaging based on the use of semiconductor quantum dots (QDs) and proton-absorbing polymeric coatings (proton sponges). With a balanced composition of tertiary amine and carboxylic acid groups, these nanoparticles are specifically designed to address longstanding barriers in siRNA delivery such as cellular penetration, endosomal release, carrier unpacking, and intracellular transport. The results demonstrate dramatic improvement in gene silencing efficiency by 10-20 fold and simultaneous reduction in cellular toxicity by 5-6 fold, when compared directly with existing transfection agents for MDA-MB-231 cells. The QD-siRNA nanoparticles are also dual-modality optical and electron-microscopy probes, allowing real-time tracking and ultrastructural localization of QDs during delivery and transfection. These new insights and capabilities represent a major step towards nanoparticle engineering for imaging and therapeutic applications.

Introduction

The ability to rationally design nanometer-sized particles with cellular delivery, imaging, and therapeutic functions is one of the most important and challenging tasks in biomedical nanotechnology.[1-7] It is expected to broadly impact a number of research areas such as molecular imaging, multiplexed profiling of disease biomarkers, and targeted therapy. Recent research has led to the development of semiconductor quantum dots (QDs) with size-tunable optical properties,[1,4,6] iron oxide nanocrystals with superparamagnetic domains,[8,9] colloidal gold nanoparticles for surface-enhanced Raman scattering (SERS),[10,11] polymeric nanostructures with drug encapsulation and release properties,[12,13] and functionalized carbon nanotubes for macromolecule delivery.[14,15] In the "mesoscopic" size range of 10-100 nm, nanoparticles also have large surface areas for linking to biorecognition ligands as well as for carrying multiple diagnostic (*e.g.*, optical, radioisotopic, or magnetic) and therapeutic (*e.g.*, anticancer) agents.

Here we report a new class of multifunctional nanoparticles for siRNA delivery and imaging based on the use of semiconductor quantum dots and proton-sponge polymer coatings. RNA

*Authors to whom correspondence should be addressed; snie@emory.edu, and xgao@u.washington.edu..

Supporting Information Available: siRNA/QD ratio determination for transfection, Electrophoresis assay of siRNA protection by QDs, control experiments without siRNA or with siRNA of random sequence, gene silencing effect and toxicity in additional cell lines, and realtime nanoparticle tracking. This material is available free of charge via the Internet at http://pubs.acs.org.

interference (RNAi) is a powerful technology for sequencespecific suppression of genes, and has broad applications ranging from functional gene analysis to targeted therapy.[16-21] However, these applications are still limited by major delivery problems in cellular entry, endosomal escape, dissociation from the carrier (that is, unpacking), and coupling with cellular machines (such as the RNA-induced silencing complex or RISC). For cellular and *in-vivo* siRNA delivery, a number of approaches have been developed (see ref. 16 for a review), but these methods have various shortcomings and do not allow a balanced optimization of gene silencing efficacy and toxicity. For example, previous work has used QDs and iron oxide nanoparticles for siRNA delivery and imaging,[21-24] but the QD probes are either mixed with conventional siRNA delivery agents[21] or an external compound such as the antimalaria drug chloroquine must be used for endosomal rupture and gene silencing activity.[22]

In this work, we have taken advantage of the versatile chemistry of polymer encapsulated QDs, and have developed multifunctional nanoparticles for highly effective and safe RNA interference by balancing two proton-absorbing (that is, proton sponge) chemical groups (carboxylic acid and tertiary amine) on the QD surface. The proton sponge effect arises from a large number of weak conjugate bases (with buffering capabilities at pH 5-6), leading to proton absorption in acid organelles and an osmotic pressure buildup across the organelle membrane.[25] This osmotic pressure causes swelling and/or rupture of the acidic endosomes and a release of the trapped materials into the cytoplasm. A major finding here is that this proton-sponge effect can be precisely controlled by partially converting the carboxylic acid groups into tertiary amines. When both are linked to the surface of nanometer-sized particles, these two functional groups provide steric and electrostatic interactions that are highly responsive to the acidic organelles, and are also well suited for siRNA binding and cellular entry. As a result, we have improved the gene silencing activity by 10-20 fold, and have simultaneously reduced the cellular toxicity by 5-6 fold in MDA-MB-231 cells (in comparison with current siRNA delivery agents such as lipofectamine, JetPEI, and TransIT). We also show that the QD-siRNA nanoparticles are dual-modality optical and EM probes, and can be used for real-time tracking and ultrastructural localization of QDs during delivery and transfection.

Methods

Reagents and instruments

Unless specified, chemicals were purchased from Sigma-Aldrich (St. Louis, MO) and used without further purification. A UV-2450 spectrophotometer (Shimadzu, Columbia, MD) and a Fluoromax4 fluorometer (Horiba Jobin Yvon, Edison, NJ) were used to characterize the absorption and emission spectra of QDs. The dry and hydrodynamic radii of QDs and QD-nanobeads were measured on a CM100 transmission electron microscope (Philips EO, Netherlands) and a Zetasizer NanoZS size analyzer (Malvern, Worcestershire, UK). True-color fluorescence images were obtained with an IX-71 inverted microscope (Olympus, San Diego, CA) and a D1 digital color camera (Nikon). Broad-band excitation in the near-UV range (330-385 nm) was provided by a mercury lamp. A longpass dichroic filter (400 nm) and emission filter (420 nm, Chroma Technologies, Brattleboro, VT) were used to reject the scattered light and to pass the Stokes-shifted fluorescence signals. Multicolor gel images were acquired with a macro-imaging system (Lightools Research, Encinitas, CA).

Synthesis of QDs and proton-sponge coatings—Highly luminescent QDs were synthesized as previously described.[26,27] Briefly, cadmium oxide (CdO, 1 mmole) precursor was first dissolved in 1 g stearic acid with heating. After formation of a clear solution, tri-noctylphosphine oxide (TOPO, 5 g) and Hexadecylamine (HDA, 5 g) mixture were added as reaction solvents, which were then heated to 250 °C under argon for 10 minutes. The reaction temperature was briefly raised to 350 °C, and equal molar selenium solution is quickly injected

into the hot solvents. The mixture immediately changes color to orange-red, indicating QD formation. The dots were refluxed for 10 minutes, and capping solution of 20 mM dimethlyzinc and hexamethlydisilathiane was slowly added to protect the CdSe core. The resulting QDs were cooled to room temperature, and were rinsed repeatedly with methanol and hexane to remove free ligands. UV adsorption, fluorescence emission spectra, Transmission Electron Microscopy (TEM), and Dynamic Light Scattering (DLS) were used for characterization of particle optical properties and sizes.

For nanoparticle encapsulation, purified QDs (100 nM) were mixed with poly-maleic anhydride-*alt*-1-tetradecene (10 μM) in chloroform, the mixture was slowly dried under vacuum over a time period of 4-8 hours. The resulting transparent thin film was sonicated in sodium carbonate buffer (pH 8.5), leading to water-soluble QDs. Excess polymer were removed by using a filtration column (first concentrated with Beckman TX-120 ultracentrifugation). For covalent grafting of carboxylic acid groups on the QD surface with tertiary amines, the QDs were first activated with N-(3-mimethylaminopropyl)-N′-ethylcarbodiimide hydrochloride (EDAC), and were then reacted with N,N-dimethylethylenediamine (10 mM). Due to EDAC's instability during storage, its amount used for crosslinking was adjusted experimentally until the final QDs reached a zeta potential of approximately 20 mV. The proton-sponge coated QDs were thoroughly purified by dialysis (MWCO 3,000) to remove unreacted amines and crosslinking reagents, and were stored at 4 ° C for use.

Cell transfection procedures—Cellular transfection by short synthetic RNA was performed using Lipofectamine 2000 (Invitrogen Corp., Carlsbad, CA), TransITTKO® (TransIT) (Mirus Bio Corp., Madison, MI), JetPEI (Qbiogene, Morgan Irvine, CA), as well as our proton-sponge coated QDs. The cell lines studied were MDA-MB-231 (breast carcinoma), MCF-7 (breast carcinoma), NIH3T3 (mouse fibroblasts), NCI-H 460 (NCI-H-lung carcinoma), PC-3 (prostate carcinoma). Cells were cultured in 75cm^2 tissue culture flasks (Cellstar®, Greiner Bio-One GmbH, Frickenhausen, Germany) with Dulbecco's modification of Eagle's medium DMEM (Invitrogen Corp., Carlsbad, CA). According to the specific medium requirements for different cell lines 5 to 10% of fetal bovine serum (FBS, Sigma, Steinheim, Germany) and 5% of penicillin - streptomycin solution (Sigma, Steinheim, Germany) were added to DMEM for optimal growth. For siRNA transfection, cells were trypsinized with 0.25% of trypsin solution for 3 min at 37^{0}C. After trypsin has been neutralized by 10% FBS solution, cells were re-suspended in medium and the cell concentration was established using a hemacytometer. Next, 3×10^4 cells per well were plated into 24-well plates (Corning Incorporated, Corning, NY) overnight to achieve 60-80% confluence. On the day of transfection, cultured cells were washed with 1x phosphate- buffered saline (PBS, Mediatech, Inc, Herndon, VA) and pre-incubated for 40 min with optimized modified Eagle's medium OptiMEM (Invitrogen Corp., Carlsbad, CA) without serum or antibiotics. Lipofectamine (2 μl/well) and TransIT (2 μl/well) were diluted in 500 μl of OptiMEM (manufacturer recommended concentrations) and were incubated for 15 min at room temperature. Then 100 nM siRNA against human cyclophilin B (Dharmacon Inc., Chicago, IL) was added to the mixture of medium and transfection agents, and incubated for additional 20 min at room temperature. For siRNA transfection with JetPEI, the transfection reagent and siRNA were separately diluted in 50 μl of sterile NaCl solution (150 nM), vortexed for 10 sec, mixed together and vortexed again for 10 sec followed by 20 min incubation at room temperature. QD-siRNA complexes were prepared by mixing the suspension of proton-sponge coated QDs with siRNA (diluted in the siRNA buffer (Dharmacon Inc., Chicago, IL)) to achieve siRNA:QD molar ratio of 2:1, which is determined to be the optimal ratio in the current study (Supporting Figure S1). The QD-siRNA complexes remain single, indicated by DLS (small size increase) and fluorescence microscopy measurements (showing as ‘blinking’ particles, a characteristics of single QDs). Immediately before transfection, 500 μl OptiMEM was added to QDs-siRNA

complexes and were mixed by pipeting. The QD-siRNA complexes diluted in OptiMEM were then added to each well, and the cells were incubated at 37 °C for 18 h. DMEM with 10% of FBS was then added to the cells and incubated for 36 h at 37 °C in a CO_2 incubator. We found that our proton-sponge coated QDs were also effective in RNA interference in serum-containing culture media at a QD:siRNA ratio of ~1:1, a significant advantage over liposome or lipid based transfection agents.

Western immunoblotting—Transfected cells were lysed using radioimmuno precipitation assay (RIPA) lysis buffer containing 1% Igepal-630, 0.5% deoxycholate, 0.1% SDS, 1 mM PMSF and 1μg/ml of each leupeptin, aprotinin and pepstatin in PBS (pH 7.6). The lysates were separated by centrifugation at 12 krpm, 0°C for 10 minutes on Eppendorf 5415R centrifuge (Eppendorf, Hamburg, Germany). Supernatants were then collected and protein concentration was measured by a standard Bradford assay (Bio-Rad laboratories, Inc. Hercules, CA). Equal amounts of protein were first loaded and separated on 11% sodium dodecyl sulfate polyacrylamide gel electrophoresis (SDS-PAGE), and were then transferred for 1 hour at 100 volts using Bio-Rad PowerPac (Bio-Rad Laboratories, Inc. Hercules, CA) to nitrocellulose membranes (Bio-Rad laboratories, Inc. Hercules, CA) in transfer buffer (25mM TrisHCl, 190mM glycine, 10% methanol) and blocked with 5% milk blocking buffer (5% of skim milk powder, EMD Chemicals, Darmstadt, Germany) for 2 hours on horizontal shaker. The blocked membranes were incubated with 1:200 rabbit polyclonal anti-human cyclophilin B antibodies diluted in 5% milk blocking buffer (Abcam, Cambridge, MA). The membranes were washed in Tween-Tris Buffered Saline (TTBS: 0.1% Tween-20 in 100 mM Tris-CL [pH 7.5], 0.9% NaCl) and probed with horseradish peroxidase (HRP)-linked labeled goat anti-rabbit secondary antibodies (Cell Signaling Inc., Beverly, MA) diluted at 1:5,000 in 5% milk blocking buffer. The blots were developed by using an ECL kit (Amersham Corp., Arlington Heights, IL). The membranes were exposed to Kodak X-OMAT film for 10 - 30 seconds for data acquisition and developed using conventional film developing machine.

Gel motility assay—Equal amounts of unmodified QDs, and proton-sponge coated QDs (545 and 625nm) were loaded into 1% acrylamide gels, and were separated by electrophoresis in TBE running buffer (45 mM Tris base, 45 mM boric acid, 1 mM EDTA, pH 8.3) at 100V for 30 min. Multicolor gel images were acquired with the macro-imaging system.

Cytotoxicity assay—Sulforhodamine B (SRB) assay was used according to the method by Skehan *et. al.*[28] Briefly, cells were collected by trypsinization, counted (as described above) and plated at a density of 10,000 cells per well in 96-well flat-bottomed microtiter plates (Corning Incorporated, Corning, NY) with 100 μl of cell suspension per well. For chemosensitivity assays, Lipo, TransIT, JetPEI and QD were tested at concentrations ranging from 0 to 10 times of the optimal transfection dose. The optimal dose was the concentration of transfection reagents recommended by the manufacturer for optimal transfection results (balanced silencing efficiency and cellular toxicity). For cytotoxicity studies, the transfection reagents were diluted in OptiMEM and were incubated for 6-48 hours with cells. After incubation cells were washed with 100μl of PBS x1, fixed with incubation for 1 hour in 50% trichloracetic acid and dyed with 100μl of 0.4% of SRB solution in 1% acetic acid. 100 μl of 10mM of unbuffered Trizma base solution (Sigma, Steinheim, Germany) was added to each cell. The optical density of treated cells which represented the amount of survived cells was determined at 540 nm wavelength on a fluorescence plate reader (SpectraMax 384 plus, Molecular Devices, Sunnyvale, CA). Each experiment was repeated for a minimum of three times.

Results and Discussion

Figure 1 shows the preparation of proton-sponge coated QDs and their multiple functions for siRNA delivery. These functions are achieved by balancing the ratio of carboxylic acid (-COOH) and tertiary amine groups (-NR_2) on the QD surface. Tertiary amines provide a positive charge for electrostatic siRNA binding and also for protecting nucleic acids from enzymatic degradation.[29-33] QD surface coatings with positive charges can also enter mammalian cells via macropinocytosis,[34,35] a fluid-phase endocytosis process that is initiated by QD binding to the cell surface. The QD-siRNA complex studied here is not cell-type or receptor specific. It's worth mentioning that the specific targeting deserves further development by combining QD-siRNA with a targeting probe (*e.g.*, peptide, antibody, or aptamer). Furthermore, clustered tertiary amines grafted on a polymer backbone have strong proton absorbing capabilities inside endosomes (pH 5-6) and lysosomes (pH 4-5), leading to rapid osmotic swelling and siRNA release. The ratio of carboxylic acid and tertiary amine groups provides a "tunable" parameter for optimizing the RNA silencing efficiency and its cellular toxicity (since in general, carboxylic acids are less toxic than amines). With less tertiary amines, the affinity between QDs and siRNA is not strong enough, whereas with more amines the cytotoxicity of QDs increases. The co-existence of carboxylic anions (-COO^-) and trtiary amine cations (-NHR^+_2) in a "zwitterion" form is an important structural feature because it weakens siRNA binding to the carrier QD and thus facilitates siRNA unpackaging. Indeed, when the QD surface contains approximately 50% carboxylic acid and 50% tertiary amine groups, only 70% of the bound siRNA are protected from nuclease degradation (Supporting Figure S2). This protection level is considerably lower than that achieved with more positively charged nanoparticles such as primary amines and quaternary-amines in the absence of carboxylic acid groups.[29-33] This reduced electrostatic binding is beneficial because it is expected to facilitate dissociation and unpacking of the siRNA-QD complexes in the cytoplasm, thus increasing the gene silencing efficiency. In agreement, Pack and coworkers[36] have found that when polyethylenimines (PEIs) are chemically modified to reduce electrostatic binding, the gene delivery activity is increased by 20-60 fold. These results indicate that siRNA binding and unpacking are both important factors for optimizing the interactions between siRNA and its carriers.

Essential to the success of QDs and other synthetic nanoparticles is a built-in mechanism for efficient siRNA escape from intracellular organelles.[37] Ratiometric imaging studies by Verkman and coworkers have shown that the proton-sponge effect leads to chloride accumulation, organelle swelling, and eventual endosomolysis.[38] Duan *et al* have also shown that QDs coated with a proton-sponge layer (PEG-modified PEI) are able to penetrate cells and to escape from intracellular organelles.[39] The QD surface ligands were replaced by the amines in PEI, a procedure that reduces QD stability and fluorescence quantum efficiency, unfortunately.[40] In this work, the proton-sponge polymer is amphiphilic, which not only keeps the original QD surface ligands but is also capable of buffering protons. In addition, Rozema and coworkers have found that polymer-siRNA conjugates with endosomolytic properties lead to efficient suppression of cholesterol synthesis upon systemic administration.[41] In the absence of proton-buffering groups, cellular entry can still occur but the delivered cargos cannot escape the intracellular organelles.[42] Specifically, we find that quantum dots coated with primary amines (including the amino acids lysine and arginine) bind to siRNA more strongly than the tertiary amine QDs, but they are largely ineffective for gene silencing. Similarly, colloidal gold nanoparticles coated with quaternary amines are poor vectors for gene delivery because the quaternary amines have no proton buffering abilities.[43] It is thus clear that the proton-sponge effect is a key feature for the QD-based delivery agents, although hydrophobic patches on the QD surface could also facilitate cellular entry and endosomal destabilization.[14,38]

The proton-sponge coated QDs have excellent optical properties and narrow size distributions, with comparable quantum yield values (45%) as that of the original dots (Figure 2). With a

QD core size of 6 nm (measured by TEM), the proton-sponge dots have hydrodynamic diameters of ~13 nm before siRNA binding and 17 nm after siRNA binding. They are positively charged with a zeta potential of +19.4 mV before siRNA binding and +8.5 mV after siRNA binding (also see the gel electrophoresis data). In comparison with cationic lipids and polymer-based siRNA transfection agents, the QD-based carriers are much smaller in size and more uniform in size distribution. The QDs bind siRNA on their exposed surfaces, which should facilitate siRNA dissociation and release. In contrast, traditional siRNA delivery agents often condense and trap siRNA in their interior space.[44,45]

To test the RNAi efficiency of proton-sponge coated QDs, we have examined the suppression of a native protein (cyclophilin B) in a human breast cancer cell line (MDAMB-231) as a model gene silencing target. Cyclophilin B is recommended as a positive silencing control in human cell lines, and is associated with secretory pathways.[46] It is abundantly expressed in most cells and knockdown of the corresponding mRNA does not affect cell viability. In comparison with three most commonly used transfection reagents, lipofectamine, TransIT-TKO and JetPEI (based on the same siRNA concentration and the optimized amount for each transfection reagent), Figure 3 shows that our siRNA-QD complexes leads to nearly complete suppression of cyclophilin B expression. The achieved silencing efficiencies are 18 times higher than the average of the other three transfection reagents. In contrast, control experiments using QDs only or QDs with scrambled RNA sequence show essentially no silencing effect on protein expression (Supporting Figure S3). These siRNA functional assays confirmed siRNA escape from endosome because the target mRNAs are mainly located in cytoplasm. Our QD-based transfection agents are also considerably less toxic, even at high nanoparticle concentrations and incubated for extended periods (Figure 4). Similar silencing and toxicity data have also been obtained with other cell lines including breast cancer MCF7, prostate cancer PC3, fibroblast NIH3T3, and lung cancer NCI-H, (Supporting Figures S4 and S5). Furthermore, it is important to note that the QD-siRNA complexes show similar silencing efficiencies in the presence of serum, whereas other transfection agents require serum-free media for best results.

To further investigate the intracellular behavior of QD-siRNA complexes, we have examined their uptake, transport, and localization in live cells using fluorescence microscopy (Figure 5). Dynamic imaging studies reveal that the QD-siRNA complexes are attached to the cell membrane immediately after mixing (less than one minute), and are observed as a bright ring around the cell. After internalization, the complexes move towards and become accumulated at a region outside the cell nucleus in 30 min to 4 hours. The QD-siRNA complexes are observed to undergo active and directional motions that are approximately three orders of magnitude faster than random diffusion.[47] Their trajectory and velocity are similar to active vesicle transport mediated by molecular motors such as dyneins and kinesins.[48,49] For real-time dynamic imaging, we have combined QDs' unique optical properties with a confocal microscope equipped with a Nipkow spinning disk and a cell line stably expressing GFP-microtubule (Supporting Figure S6). The results reveal that the QD and GFP signals are often colocalized, indicating that the QDs carriers move along GFP-tagged microtubules.

To confirm the role of cytoskeletons in QD transport, we treated the cells with two cytoskeleton-disrupting drugs (cytochalasin to disrupt actins, and nocodazole to disrupt microtubules). Cytochalasin had no apparent effect on the transport behavior when added independently; whereas nocodazole almost completely abolished the fast and directional movement within 1 hour. When the two drugs were added together, nocodazole took effect faster and the nanoparticles stopped moving within 30 min. These results indicate that microtubules are involved in the active transport of QDs inside living cells, while actins are likely involved in the initial uptake of QDs.[34,35] We have further studied these processes by using high-resolution TEM, and the data clearly supports the endocytosis mechanism for QD-siRNA uptake (Figure 6). Over longer periods, the vesicles entered cells and merged to form

large multivesicular structures. The QD particles were not scattered in the cytoplasm, but were clustered and attached to the organelle membranes, apparently due to electrostatic interactions between the positively charged QDs (especially after siRNA release) and the negatively charged membranes. At the present, the significance of active intracellular transport is still not clear, although RNA binding and silencing proteins such as RISC have been reported to localize in perinuclear regions called P-bodies.[50,51]

Conclusion

In conclusion, we have developed QDs as a new class of nanometer-sized scaffolds for designing multifunctional nanoparticles, and have achieved 10-20 fold improvement in gene silencing efficiency and 5-6 fold reduction in cellular toxicity. A major finding is that a proton-sponge layer formed by covalent grafting of tertiary amine groups on the QD surface leads to efficient siRNA release from intracellular vesicles. We have also shown that the QD-siRNA nanoparticles are dual-modality optical and EM probes, allowing for real-time tracking and ultrastructural localization of QDs during delivery and transfection. For in-vivo gene silencing and targeted siRNA therapy, we envision the development of nontoxic iron oxide and polymeric nanoparticles with similar proton-sponge coatings for cellular targeting, entry, and intracellular endosomal release. For rational design purposes, the measurement of siRNA activity provides a functional assay for evaluating and optimizing the performance of imaging and therapeutic nanoparticles.

Supplementary Material

Refer to Web version on PubMed Central for supplementary material.

Acknowledgements

This work was supported in part by NIH grants (P20 GM072069, R01 CA108468, U01HL080711, U54CA119338, and R01 CA131797) awarded to Profs. Nie and Gao. We also thank the Georgia Cancer Coalition for the Distinguished Cancer Scholars Program (S.N.), the University of Washington for Faculty Startup Funds (X.G.), and the NSF for Faculty Early Career Development Award (CAREER) (X.G.). We are also grateful to Dr. Adam Marcus (WCI, Emory U.) and Dr. Greg Martin (U. Washington Keck Imaging Center) for help with confocal microscopy, and Dr. Hong Yi for transmission electron microscopy.

References

1. Alivisatos P. Nat. Biotechnol 2004;22:47–52. [PubMed: 14704706]
2. Ferrari M. Nat. Rev. Cancer 2005;5:161–171. [PubMed: 15738981]
3. Niemeyer CM. Angew. Chem. Int. Edit 2001;40:4128–4158.
4. Michalet X, Pinaud FF, Bentolila LA, Tsay JM, Doose S, Li JJ, Sundaresan G, Wu AM, Gambhir SS, Weiss S. Science 2005;307:538–544. [PubMed: 15681376]
5. Rosi NL, Mirkin CA. Chem. Rev 2005;105:1547–1562. [PubMed: 15826019]
6. Gao XH, Yang L, Petros JA, Marshall FF, Simons JW, Nie SM. Curr. Opin. Biotechnol 2005;16:63–72. [PubMed: 15722017]
7. Nie SM, Xing Y, Kim GJ, Simons JW. Annu. Rev. Biomed 2007;9:257–288.
8. Harisinghani MG, Barentsz J, Hahn PF, Deserno WM, Tabatabaei S, vande Kaa CH, de la Rosette J, Weissleder R. N. Engl. J. Med 2003;348:2491–2499. [PubMed: 12815134]
9. Lee JH, Huh YM, Jun YW, Seo JW, Jang JT, Song HT, Kim S, Cho EJ, Yoon HG, Suh JS, Cheon J. Nat. Med 2007;13:95–99. [PubMed: 17187073]
10. Doering WE, Nie SM. Anal. Chem 2003;75:6171–6176. [PubMed: 14615997]
11. Nie SM, Emery SR. Science 1997;275:1102–1106. [PubMed: 9027306]
12. Torchilin VP. Pharm. Res 2007;24:1–16. [PubMed: 17109211]
13. Duncan R. Nat. Rev. Cancer 2006;6:688–701. [PubMed: 16900224]

14. Liu Z, Winters M, Holodniy M, Dai HJ. Angew. Chem. Int. Edit 2007;46:2023–2027.
15. Kam NW, Liu Z, Dai H. J. Am. Chem. Soc 2005;127:12492–12493. [PubMed: 16144388]
16. Kim DH, Rossi JJ. Nat. Rev. Genetics 2007;8:173–182. [PubMed: 17304245]
17. Rana TM. Nat. Rev. Mol. Cell Biol 2007;8:23–36. [PubMed: 17183358]
18. Bumcrot D, Manoharan M, Koteliansky V, Sah DW. Nat. Chem. Biol 2006;2:711–719. [PubMed: 17108989]
19. Meister G, Tuschl T. Nature 2004;431:343–349. [PubMed: 15372041]Dorsett Y, Tuschl T. Nat. Rev. Drug Disc 2004;3:318–329.
20. Dykxhoorn DM, Lieberman J. Ann. Rev. Med 2005;56:401–423. [PubMed: 15660519]
21. Chen AA, Derfus AM, Khetani SR, Bhatia SN. Nuc. Acids Res 2005;33:e190.
22. Derfus AM, Chen AA, Min DH, Ruoslahti E, Bhatia SN. Bioconjugate Chem 2007;18:1391–1396.
23. Tan WB, Jiang S, Zhang Y. Biomaterials 2007;28:1565–1571. [PubMed: 17161865]
24. Medarova Z, Pham W, Farrar C, Petkova V, Moore A. In vivo imaging of siRNA delivery and silencing in tumors. Nat. Med 2007;13:372–377. [PubMed: 17322898]
25. Boussif O, Lezoualc'h F, Zanta MA, Merqny MD, Scherman D, Demeneix B, Behr JP. Proc. Natl. Acad. Sci. U.S.A 1995;92:7297–7301. [PubMed: 7638184]
26. Peng ZA, Peng X. J. Am. Chem. Soc 2001;123:183–184. [PubMed: 11273619]
27. Qu LH, Peng ZA, Peng X. Nano Lett 2001;1:333–337.
28. Skehan P, Storeng R, Scudiero D, Monks A, McMahon J, Vistica D, Warren JT, Bokesch H, Kenney S, Boyd MR. J. Natl. Cancer Inst 1990;82:1107–1112. [PubMed: 2359136]
29. He XX, Wang K, Tan W, Liu B, Lin X, He C, Li D, Huang S, Li J. J. Am. Chem. Soc 2003;125:7168–7169. [PubMed: 12797777]
30. McIntosh CM, Esposito EA 3rd, Boal AK, Simard JM, Martin CT, Rotello VM. J. Am. Chem. Soc 2001;123:7626–7629. [PubMed: 11480984]
31. Fischer NO, McIntosh CM, Simard JM, Rotello VM. Proc. Natl. Acad. Sci. U.S.A 2002;99:5018–5023. [PubMed: 11929986]
32. Bharali DJ, Klejbor I, Stachowiak EK, Dutta P, Roy I, Kaur N, Bergey EJ, Prasad PN, Stachowiak MK. Proc. Natl. Acad. Sci. USA 2005;102:11539–11544. [PubMed: 16051701]
33. Chavany C, Saison-Behmoaras T, Ledoan T, Puisieux F, Couvreur P, Helene C. Pharm. Res 1994;11:1370–1378. [PubMed: 7816773]
34. Conner SD, Schmid SL. Regulated portals of entry into the cell. Nature 2003;422:37–44. [PubMed: 12621426]
35. Kaplan IM, Wadia JS, Dowdy SF. J. Control. Release 2005;102:247–253. [PubMed: 15653149]
36. Gabrielson NP, Pack DW. Biomacromolecules 2006;7:2427–2435. [PubMed: 16903692]
37. Pack DW, Hoffman AS, Pun S, Stayton PS. Nat. Rev. Drug Discov 2005;4:581–593. [PubMed: 16052241]
38. Sonawane ND, Szoka FC, Verkman AS. J. Biol. Chem 2003;278:44826–44831. [PubMed: 12944394]
39. Duan H, Nie SM. J. Am. Chem. Soc 2007;129:3333–3338. [PubMed: 17319667]
40. Smith AM, Dave SR, Nie S, True L, Gao XH. Expert Rev. Mol. Diagn 2006;6:231–244. [PubMed: 16512782]
41. Rozema DB, Lewis DL, Wakefield DH, Wong SC, Klein JJ, Roesch PL, Bertin SL, Reppen TW, Chu Q, Blokhin AV, Hagstrom JE, Wolff JA. Proc. Natl. Acad. Sci. U.S.A 2007;104:12982–12987. [PubMed: 17652171]
42. Alexis F, Lo SL, Wang S. Adv. Mater 2006;18:2174.
43. Sandhu KK, McIntosh CM, Simard JM, Smith SW, Rotello VM. Bioconjug. Chem 2002;13:3–6. [PubMed: 11792172]
44. Oberle V, Bakowsky U, Zuhorn IS, Hoekstra D. Biophys. J 2000;79:1447–1454. [PubMed: 10969006]
45. Dash PR, Toncheva V, Schacht E, Seymour LW. J. Control. Release 1997;48:269–276.
46. Price ER, Jin M, Lim D, Pati S, Walsh CT, Mckeon FD. Proc. Natl. Acad. Sci. USA 1994;91:3931–3935. [PubMed: 7909608]

47. Suh J, Wirtz D, Hanes J. Proc. Natl. Acad. Sci. U.S.A 2003;100:3878–3882. [PubMed: 12644705]
48. Burgess SA, Walker ML, Sakakibara H, Knight PJ, Oiwa K. Nature 2003;421:715–718. [PubMed: 12610617]
49. Schliwa M, Woehlke G. Nature 2003;422:759–765. [PubMed: 12700770]
50. Sen GL, Blau HM. Nat. Cell Biol 2005;7:633–636. [PubMed: 15908945]
51. Liu J, Valencia-Sanchez MA, Hannon GJ, Parker R. Nat. Cell Biol 2005;7:719–723. [PubMed: 15937477]

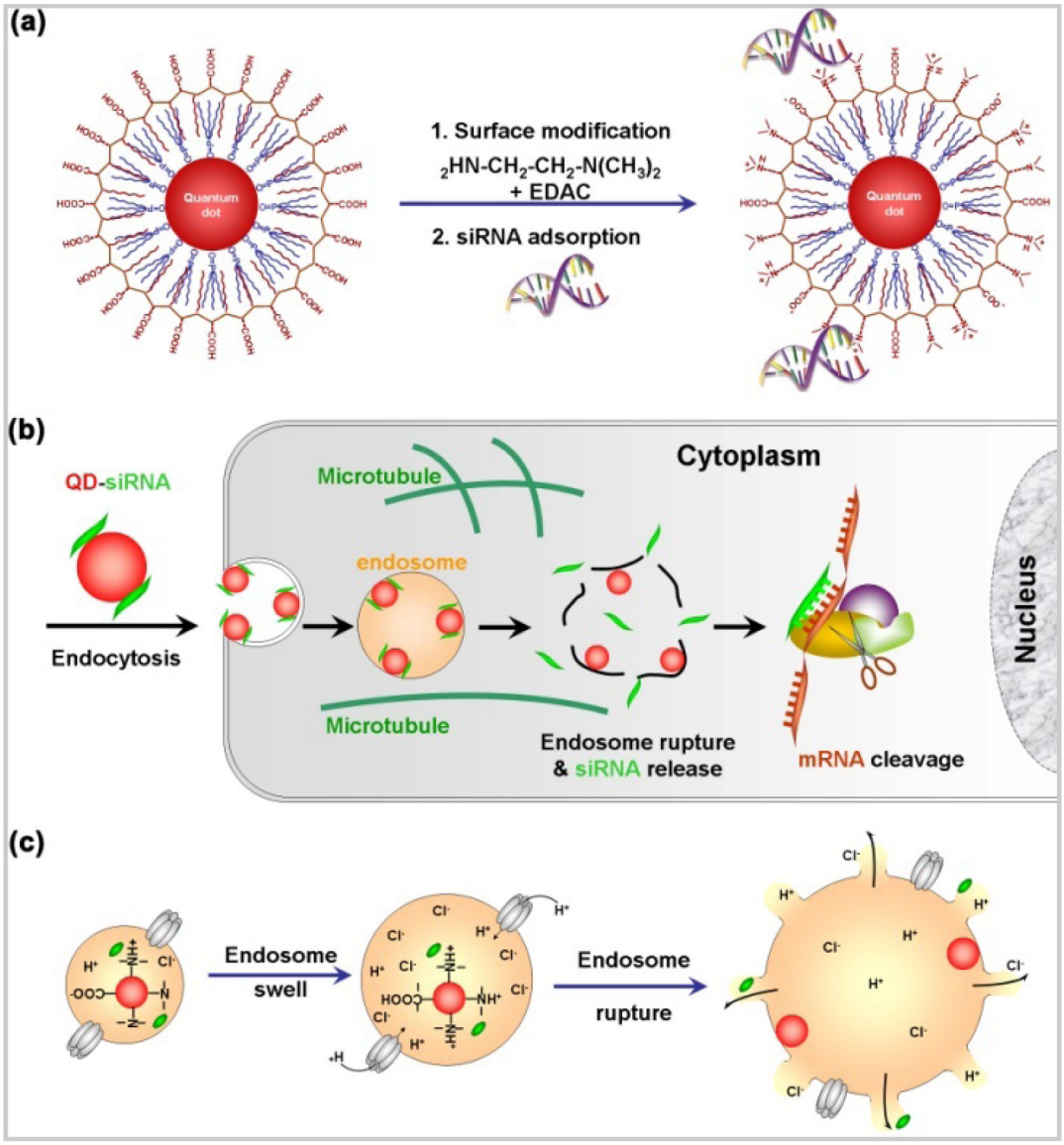

Figure 1.

Rational design of proton-sponge coated quantum dots and their use as a multifunctional nanoscale carrier for siRNA delivery and intracellular imaging. (a) Chemical modification of polymer-encapsulated QDs to introduce tertiary amine groups, and adsorption of siRNA on the particle surface by electrostatic interactions. (b) Schematic diagram showing the steps of siRNA-QD in membrane binding, cellular entry, endosomal escape, capturing by RNA binding proteins, loading to RNA-induced silencing complexes (RISC), and target degradation. (c) Schematic illustration of the proton-sponge effect showing the involvement of the membrane protein ATPase (proton pump), osmotic pressure buildup, and organelle swelling and rupture. For optimized silencing efficiency and cellular toxicity, the QD surface layer is composed of 40% (molar) carboxylic acids and 60% tertiary amines. The optimal number of siRNA molecules per particle is approximately 2 (as shown in the diagram).

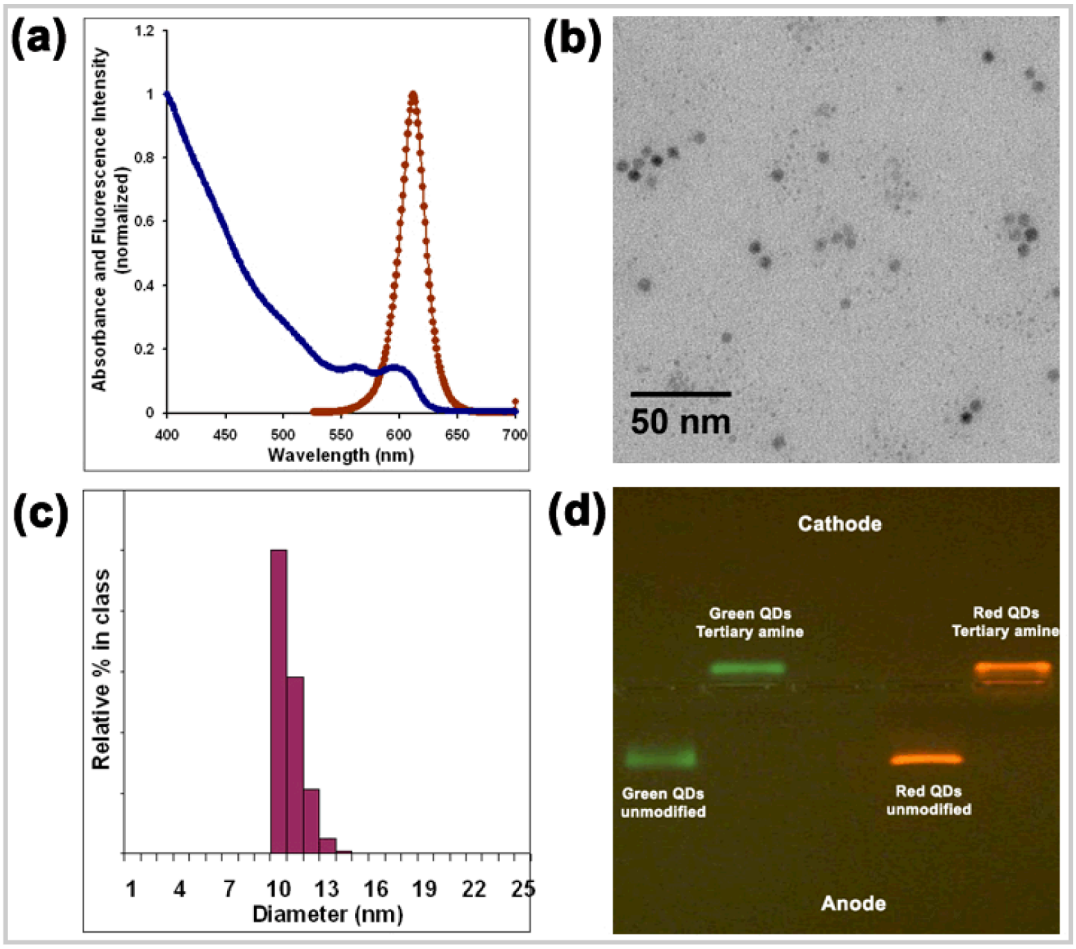

Figure 2.

Size, charge, and optical properties of proton-sponge coated QDs. (a) Optical absorption and emission spectra; (b) core size measured by transmission electron microscopy (TEM); (c) hydrodynamic size measured by dynamic light scattering; and (d) surface charges of unmodified and proton-sponge coated QDs (green 545 nm and red 620 nm) as measured by gel electrophoresis. The current separation resolution is not sufficient to show motility difference between the green and red QDs, because the sizes of polymer-coated QDs are greatly determined by the polymer layer. Nevertheless, the gel image clearly shows the opposite surface charge between original and modified QDs. With longer running distance, the differential motility between multiple colors should be distinguishable. For the red QD of 6 nm core (measured by TEM), the proton-sponge dots have hydrodynamic diameters of ~13 nm before siRNA binding and 17 nm after siRNA binding. They are positively charged with a zeta potential of +19.4 mV before siRNA binding and +8.5 mV after siRNA binding.

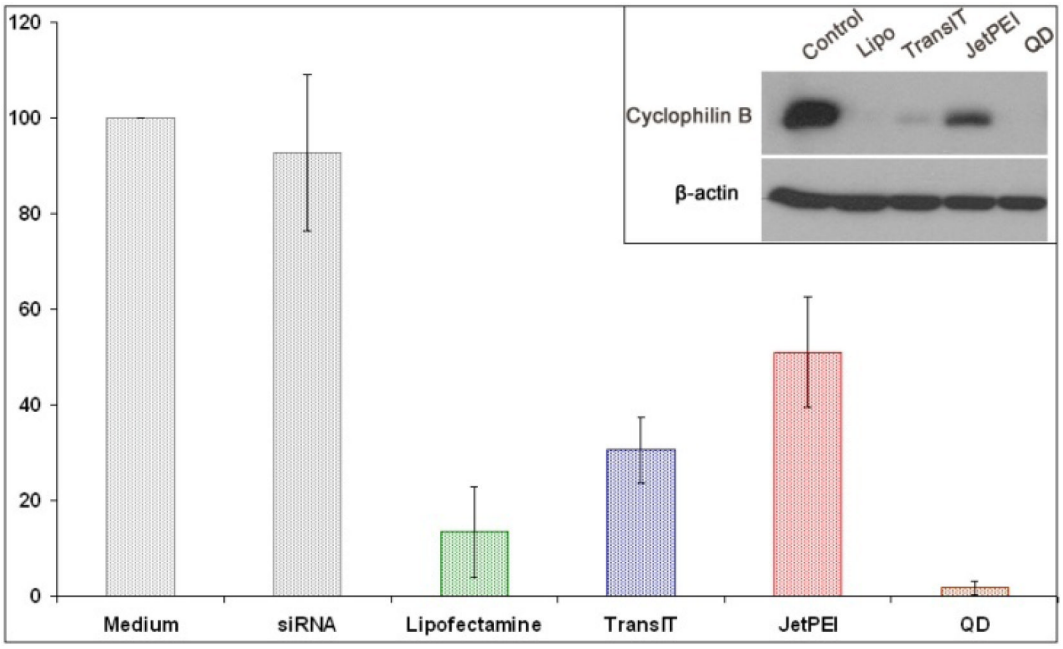

Figure 3.

Comparison of gene silencing efficiencies between proton-sponge coated QDs and commercial transfection reagents by western blotting. The level of cyclophilin B protein expression was reduced to 1.81%±1.47% by QDs, to 13.45%±9.48% by Lipofectamine, to 30.58%±6.90% by TransIT, and to 51.00%±11.46% by JetPEI (corresponding to efficiency improvements of 7.4, 16.9, and 28.2 fold, respectively). The quantitative values were obtained from the western blot (inset). On the average, the proton-sponge coated QDs are 18 times as efficient as the three transfection agents commonly used.

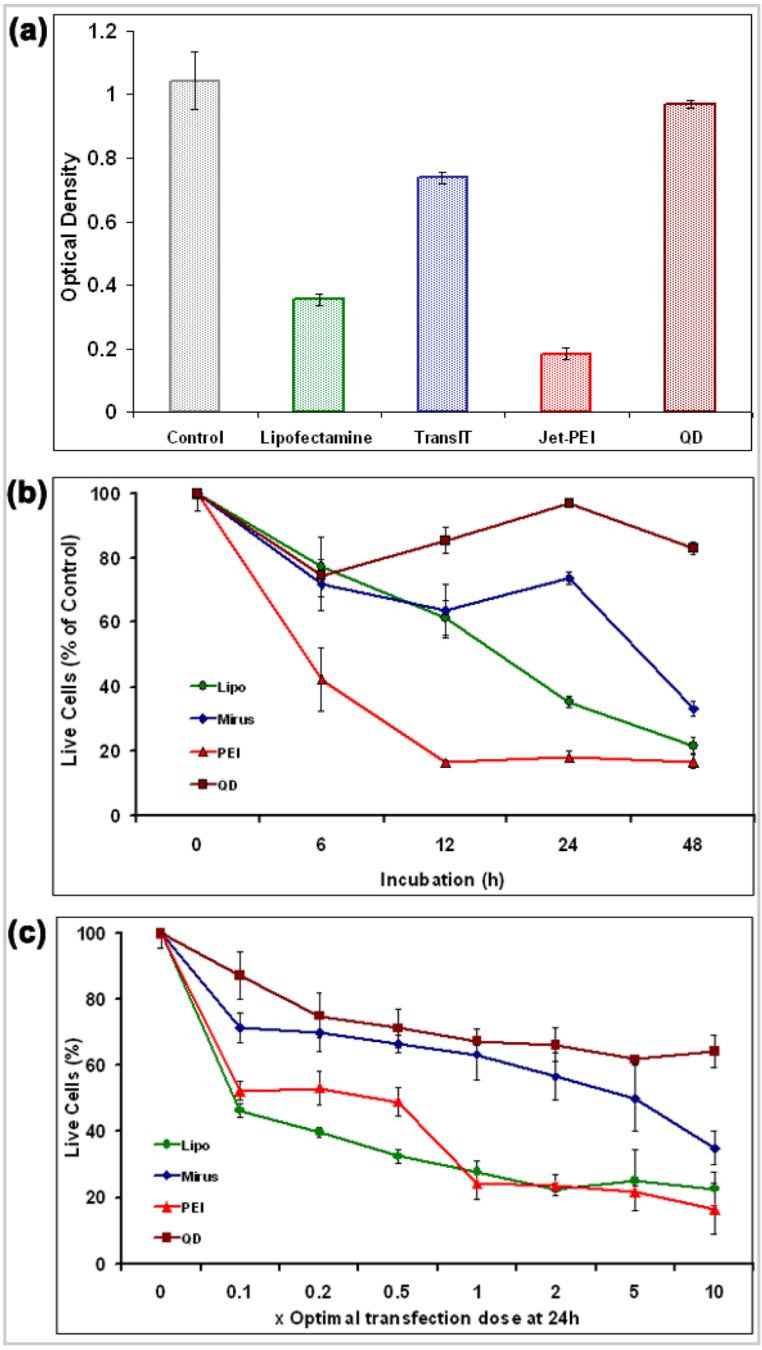

Figure 4.

Comparison of cellular toxicity between proton-sponge coated QDs and commercial transfection reagents using the SRB assay. (a) Cytotoxicity data obtained from QDs and three transfection reagents (Lipofectamine 2000, TransIT, and JetPEI) at their optimal transfection efficiencies (100 nM for QDs, see Methods for details). Data points were obtained at 24 hours, and the proton-sponge coated QDs were nearly non-toxic to MDAMB-231 cells. (b) Cellular toxicity data as a function of transfection time obtained from QDs and conventional reagents at siRNA concentrations for optimal transfection efficiency. Note that the QD-based agents performed especially well for extended transfection times. (c) Dose-dependent toxicity data for QDs and conventional agents. The x-axis indicates the fold of siRNA concentration relative

to the optimal concentration for transfection. The QD agents performed much better than other transfection agents when the siRNA concentrations were 5-10 times higher than the optimal concentration.

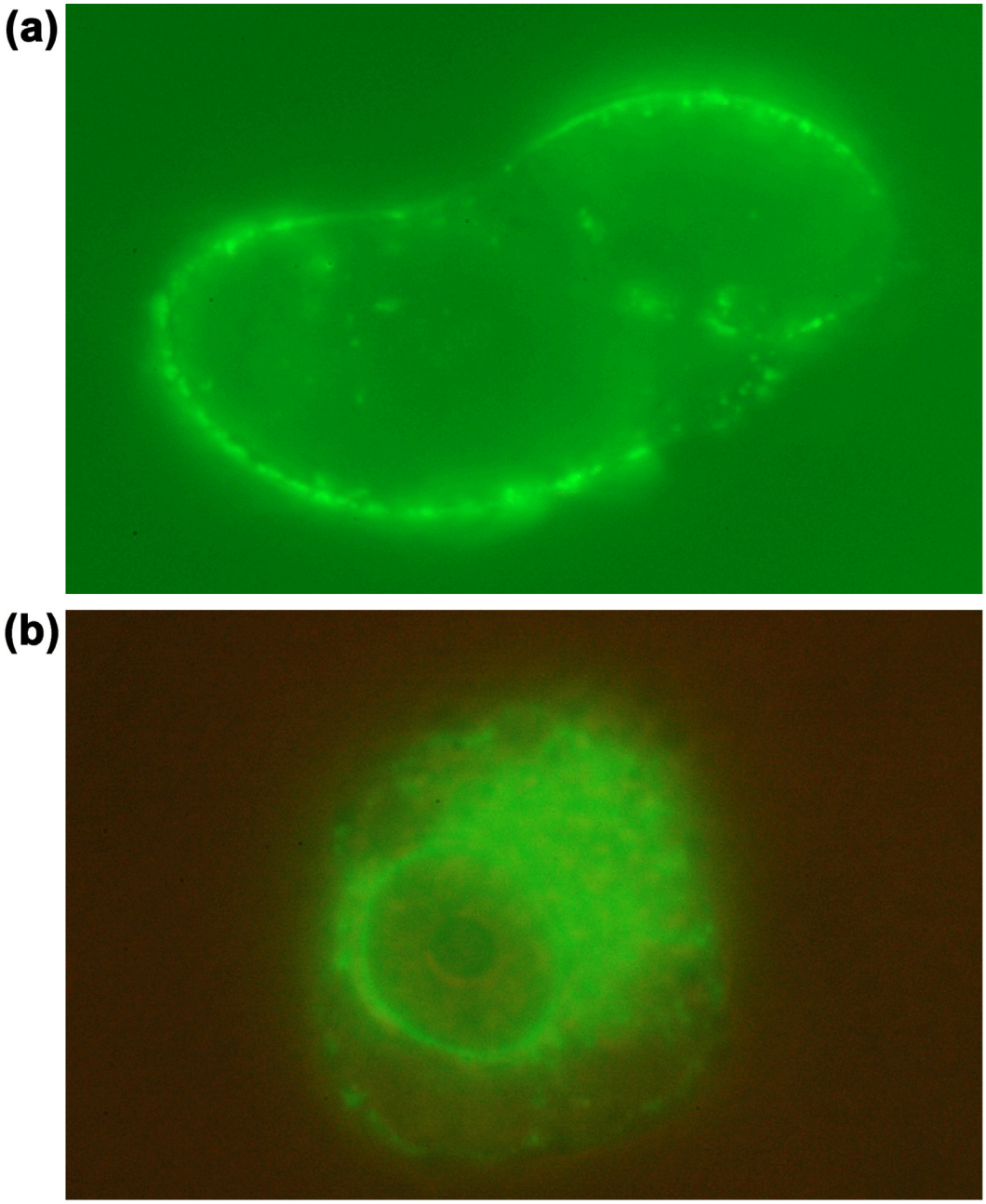

Figure 5.
Time-dependent fluorescence imaging of QD-siRNA nanoparticle conjugates and their entry and transport in living cells. Fluorescence micrographs of MDA-MB 231 cells obtained at (a) 15 min, and (b) 4 hours after the addition of QD-siRNA. The images show that at early incubation, the QD fluorescence is limited to the cell membrane, whereas extended incubation allows cytoplasm localization.

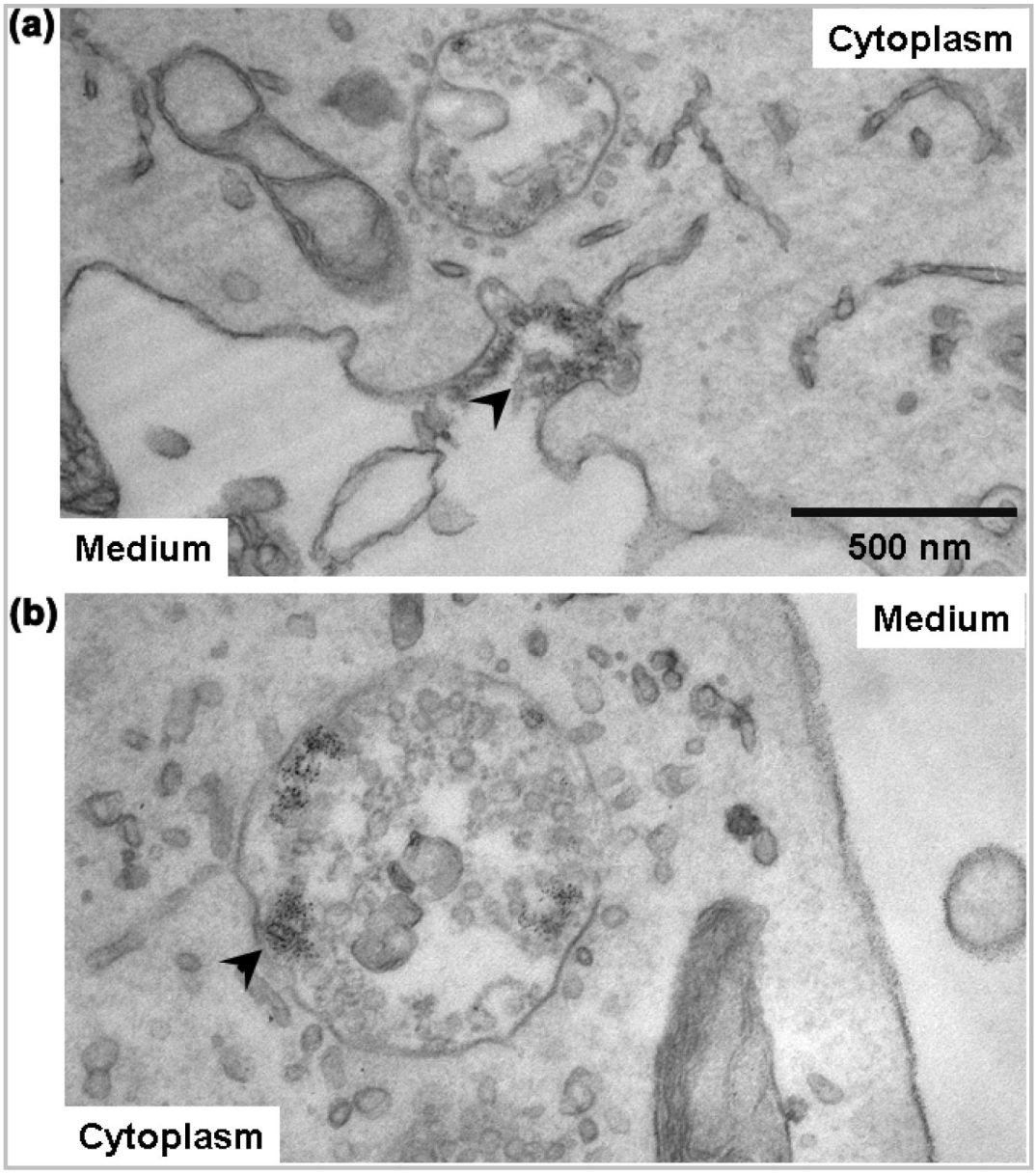

Figure 6.
Ultrastructural localization of QDs inside MDA-MB-231 cells by transmission electron microscopy (TEM). (a) TEM micrograph showing the process of siRNA-QD endocytosis and the formation of an endosome just about to enter the cell. (b) TEM micrograph showing a large multivesicular structure, QD clustering, and QD attachment to the inner vesicle membrane.